MICROBIOLOGY

Natural flavonoids disrupt bacterial iron homeostasis to potentiate colistin efficacy

Zi-xing Zhong[1,2], Shuang Zhou[1,2], Yu-jiao Liang[1,2], Yi-yang Wei[1,2], Yan Li[1,2], Teng-fei Long[1,2], Qian He[1,2], Meng-yuan Li[1,2], Yu-feng Zhou[1,2], Yang Yu[1,2], Liang-xing Fang[1,2], Xiao-ping Liao[1,2], Barry N. Kreiswirth[3], Liang Chen[3], Hao Ren[1,2]*, Ya-hong Liu[1,2,4]*, Jian Sun[1,2]*

In the face of the alarming rise in global antimicrobial resistance, only a handful of novel antibiotics have been developed in recent decades, necessitating innovations in therapeutic strategies to fill the void of antibiotic discovery. Here, we established a screening platform mimicking the host milieu to select antibiotic adjuvants and found three catechol-type flavonoids—7,8-dihydroxyflavone, myricetin, and luteolin—prominently potentiating the efficacy of colistin. Further mechanistic analysis demonstrated that these flavonoids are able to disrupt bacterial iron homeostasis through converting ferric iron to ferrous form. The excessive intracellular ferrous iron modulated the membrane charge of bacteria via interfering the two-component system *pmrA*/*pmrB*, thereby promoting the colistin binding and subsequent membrane damage. The potentiation of these flavonoids was further confirmed in an in vivo infection model. Collectively, the current study provided three flavonoids as colistin adjuvant to replenish our arsenals for combating bacterial infections and shed the light on the bacterial iron signaling as a promising target for antibacterial therapies.

INTRODUCTION

Antibiotics have been widely applied for nearly 100 years since Alexander Fleming heralded the antibiotic era (*1*). Regrettably, the cumulative consumption of antibiotics has led to the emergence and spread of antibiotic resistance at an alarmingly high rate (*2*, *3*). To date, numerous transferable antibiotic resistance genes have been identified, including those conferring resistance to last-resort antibiotics such as carbapenem, colistin, and tigecycline (*4*–*6*). The looming crisis of antimicrobial resistance (AMR) threatens current treatment paradigms based on antibiotics, presenting a worrisome scenario where some bacterial infections that were once easily treatable are now deadly. Clinical antibiotic choices are mainly guided by the antimicrobial susceptibility testing (AST) results, primarily based on minimum inhibitory concentration (MIC) values. However, AST of commonly prescribed antibiotics is often tested in vitro in universal medium, which does not always correlate with the clinical treatment efficacy in vivo. In addition, standard AST, sometimes, inadvertently excludes antibiotics with potent efficacy, due to their high MIC values, despite being synergistic with other antibiotics (*7*). In concert with the rising antibiotic resistance, the traditional source of antibiotic seems to be overmined, as the discovery of novel antibiotics lags far behind the rapid evolution and dispersion of antibiotic resistances (*8*). Therefore, more innovative strategies must be included to bridge the gap between the availability of new therapy and increasing AMR concerns.

Such innovations, exemplified by combinatorial therapy, drug repurposing, antiviral therapy, rational optimization of leads, and new leads development from untapped source, have profoundly expanded our arsenal to combat the infections caused by resistant bacteria (*9*–*11*). It is notably that all these strategies have pros and cons, and their cost, efficacy, and biosafety should be considered before their introduction to clinical practice. In comparison to the discovery of new antimicrobial leads, the combination strategy offers a promising approach to revitalize existing antibiotics with well-researched and clinically validated status (*12*). One best example is the syncretic combination of β-lactam antibiotics with β-lactamase inhibitors like clavulanate and avibactam, which have been used to target extended spectrum β-lactamase and carbapenemase-producing bacteria (*13*). Besides the combination of antibiotic with target-specific inhibitors, a short linear antibacterial peptide S25 (SLAP-25), with broad-spectrum adjuvant property, was also reported to be able to potentiate the efficacies of tetracycline, ofloxacin, rifampicin, cefepime, and vancomycin (*14*). Thus, these examples underscore the promising feasibility of combination therapy to overcome the antibiotic resistance.

Among the antibiotic of last resort, colistin has been deemed as a viable therapeutic option to eradicate multidrug-resistant (MDR) bacteria, especially carbapenem-resistant *Enterobacteriales* (*15*, *16*). Although colistin demonstrates a rapid bacterial clearance, its in vivo efficacy has always being suboptimal, as up to 70% of patients responded poorly to colistin treatment (*17*–*20*). It suggested that the pathogens at host sites may respond differently to colistin at regular doses. However, using colistin in excess is also not possible due to its nephrotoxicity (*21*). Unfortunately, the situation has been exacerbated by the emergence of chromosome-mediated and mobile element–mediated colistin resistance (e.g., Mcr-1), which confer colistin resistance by modulating membrane charge (*4*). In the face of such intrinsic or acquired colistin resistance, current

[1]Guangdong Laboratory for Lingnan Modern Agriculture, National Risk Assessment Laboratory for Antimicrobial Resistance of Animal Original Bacteria, College of Veterinary Medicine, South China Agricultural University, Guangzhou 510642, PR China. [2]Guangdong Provincial Key Laboratory of Veterinary Pharmaceutics, Development and Safety Evaluation, South China Agricultural University, Guangzhou 510642, PR China. [3]Hackensack-Meridian Health Center for Discovery and Innovation, Nutley, NJ, USA. [4]Jiangsu Co-Innovation Center for the Prevention and Control of Important Animal Infectious Diseases and Zoonoses, Yangzhou University, Yangzhou 225009, PR China.
*Corresponding author. Email: hao.ren@scau.edu.cn (H.R.); gale@scau.edu.cn (Y.-h. L.); jiansun@scau.edu.cn (J.S.)

colistin treatment necessitates innovative strategies to enhance colistin efficacy for better clinical outcomes. To this end, a panel of colistin adjuvants has been developed in previous studies. Liu and co-workers (*22*) identified that melatonin, a neurohormone, resensitize the Gram-negative bacteria to colistin by targeting the bacterial membrane and promoting oxidative damage. In a recent report, De Oliveira *et al.* (*23*) repurposed an ionophore for neurodegenerative disease, PBT-2, to break the resistance to polymyxin by disrupting bacterial intracellular metal homeostasis to a larger extent. In addition, silver was found to substitute the essential zinc ion in the intact enzyme of MCR, to curb the *mcr-1*–mediated colistin resistance in vitro and in vivo (*24*). These efforts demonstrated that combinations of colistin with rational adjuvants are of great potential to enhance current treatment paradigms based on colistin.

Here, we established a screening platform based on host-mimicking condition, in which three natural catechol-type flavonoids that synergized with colistin were selected. The three flavonoids substantially potentiated colistin efficacy against both colistin-sensitive and colistin-resistant isolates. Our mechanistic analysis demonstrated that these flavonoids disrupt bacterial iron homeostasis, dysregulating the iron signaling to promote colistin binding on bacterial membrane and subsequent accumulation of reactive oxygen species (ROS). Collectively, the current study unveiled the great potential of these catechol-type flavonoids as colistin adjuvants and highlighted iron signaling as an ideal target for colistin treatment.

RESULTS

Primary screening identified catechol-type flavonoids as adjuvants to colistin

The suboptimal clinical response of colistin in vivo has revealed that the resistances against polymyxin antibiotic can also be conferred to Gram-negative bacteria by intrinsic mechanism under defined host conditions (*25*). Therefore, we sought to establish a screening method that mimics the host condition to more precisely select adjuvants that can potentiate colistin efficacy in vivo. To this end, we adopted the low-phosphate, low-magnesium media (LPM) medium (*26*), which was constructed to resemble the condition in macrophage (Fig. 1A). The colistin MIC of *Salmonella typhimurium* strain ATCC14028s (*S.* Tm str. 14028s, colistin-sensitive) in LPM was 16-fold higher than that from the Mueller Hinton (MH) medium, likely due to the acidification and magnesium unavailability in macrophage-mimicking conditions (table S1). Subsequently, a total of 37 phytochemicals were screened according to a previous method using the LPM medium (*27*). The growth profiles [optical density at 600 nm (OD_{600nm})] of bacteria in the presence of colistin, phytochemicals, or their combinations relative to that of no-drug control were presented as W_X, W_Y, and W_{XY}, respectively. The $\tilde{\varepsilon}$ value for defining the interaction between colistin and phytochemicals was introduced as $(W_{XY} - W_X W_Y)/(\tilde{W}_{XY} - W_X W_Y)$, where $\tilde{W}_{XY}$ was equal to min $[W_X, W_Y]$ for $W_{XY} > W_X W_Y$ and 0 otherwise. The $\tilde{\varepsilon}$ value of −0.5 was set as a cutoff to select the potential compounds that synergize with colistin. The primary screening identified three hits (8.1%) as lead compounds that could potentiate colistin in LPM (Fig. 1B and table S2).

Intriguingly, the three hits were all flavonoids and shared the same modification of catechol (1,2-dihydroxy benzene) moiety. Hence, we hypothesized that the catechol moiety might be vital for the activity of these compounds. To address this hypothesis, a structure-activity relationship (SAR) analysis was conducted by comparing the activities of catechol-type flavonoids to their derivatives without the catechol-type flavonoids (Fig. 1C). As shown in Fig. 1D, the catechol-type flavonoids, including 7,8-dihydroxyflavone (7,8-DHF), myricetin (MYR), and luteolin (LUT), profoundly restored the colistin sensitivity against bacteria, yet no synergy was observed on the resorcinol-type flavonoids (5,7-DHF) and hydroxyflavone (7-HF and 8-HF). Further details were given in fig. S1. Together, these findings suggest that the three catechol-type flavonoids identified in our primary screening are promising adjuvants to restore colistin activity in host-mimicking condition.

Candidate flavonoids restore colistin activity against chromosome and plasmid-mediated colistin-resistant bacteria and minimize the emergence of resistance

With findings that three candidate flavonoids were able to potentiate colistin efficacy, we next determined whether these combinations are also effective against the colistin-resistant bacteria bearing *mcr* genes or chromosomal *mgrB* mutation. The tests were performed on four representative MDR isolates of Gram-negative bacteria: *mcr-1*–positive 17ES (*S. typhimurium*), 2012FS (*Escherichia coli*), CMG (*Klebsiella pneumoniae*), and an *mgrB*-disrupted ZJ18-19 (*K. pneumoniae*). As illustrated in isobolograms, a typical synergistic effect between the candidate flavonoids and the colistin was observed with fractional inhibitory concentration index (FICI) ranging from 0.125 ± 0 to 0.458 ± 0.072 (Fig. 2A and fig. S2). To reinforce the notion of synergism between the candidate flavonoids and colistin, a direct synergistic bactericidal assay was conducted on the aforementioned colistin-resistant strains. In the monotherapy assay, the application of colistin, 7,8-DHF, MYR, and LUT could hardly kill the bacteria over time. In contrast, the combination of colistin plus any of the three candidate flavonoids rapidly eradicated the colistin-resistant strains, and the bacterial loads were reduced by 10^2- to 10^5-fold after treatments (Fig. 2B and fig. S3).

To gain the insights on resistance development, both colistin-sensitive and colistin-resistant strains (*S.* Tm str. 14028s, 17ES, and ZJ18-19) were serially passaged in the medium supplemented with colistin with or without candidate flavonoids. The development of resistance to colistin was observed to be reduced by the application of candidate flavonoids in three tested strains, whereas the colistin alone rapidly resulted in an increment of MIC up to eightfold (Fig. 2C). These results collectively suggested that the synergistic combinations of colistin with 7,8-DHF, MYR, and LUT were an efficient approach to eliminate the bacteria and minimize the potential emergence of resistance.

Candidate flavonoids target bacterial iron homeostasis to synergize with colistin

In view of the promising synergism between 7,8-DHF, MYR, and LUT with colistin, we sought to determine the underlying mechanisms. We first performed the RNA sequencing (RNA-seq) on the bacteria treated with single colistin or colistin in combination with 7,8-DHF, as a representative candidate of flavonoid. Transcriptomic data revealed that a total of 647 genes were differentially regulated after the treatment of the flavonoid-colistin combination compared with cells treated by colistin alone (fig. S4). The Gene Ontology (GO) enrichment analysis demonstrated that the differentially

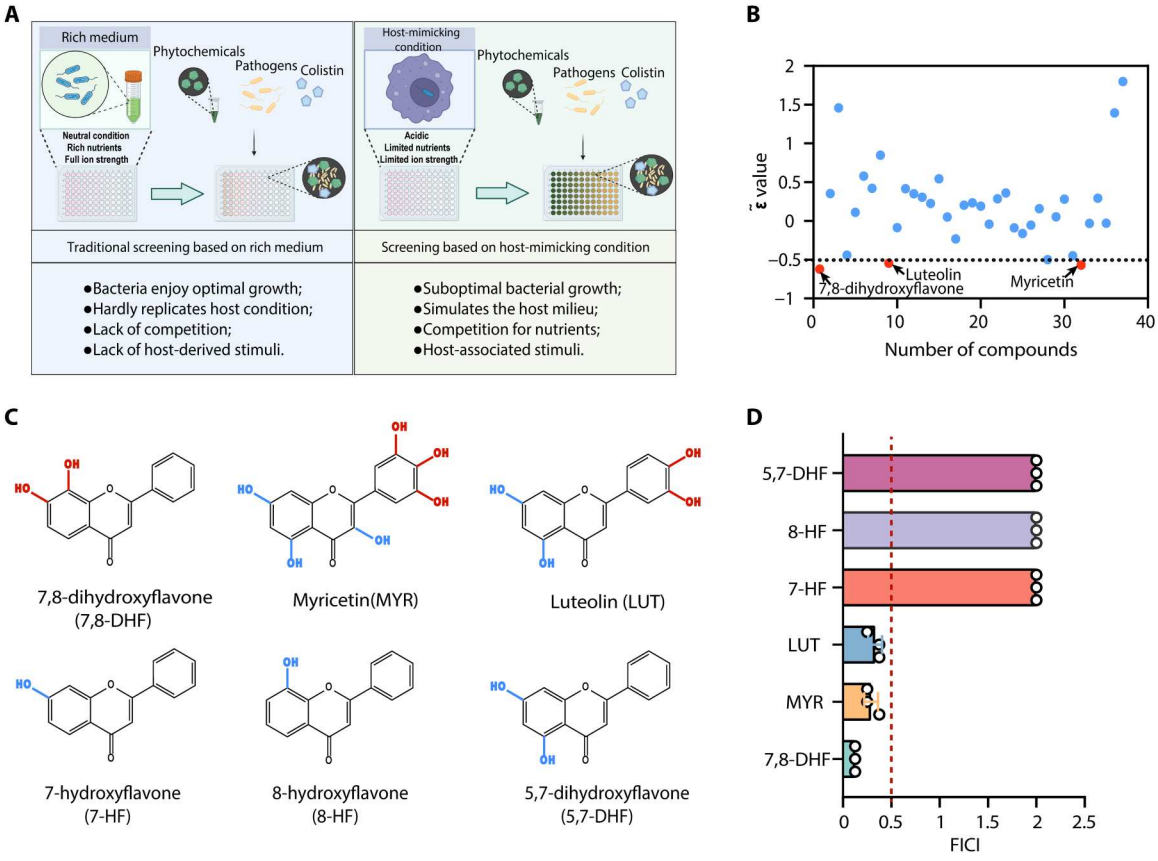

Fig. 1. Primary screening identified three catechol-type flavonoids as colistin adjuvants. (**A**) Schematic illustration of the screening procedure. (**B**) Three flavonoids were identified as potent colistin adjuvants from the phytochemical collection. (**C**) Structure-activity relationship (SAR) analysis demonstrated the presence of catechol moiety on flavonoids as a prerequisite for observed synergy. (**D**) Fractional inhibitory concentration indices (FICIs) showing the combination between colistin and catechol-type/non–catechol-type flavonoids.

expressed genes (DEGs) were highly associated with several pathways in biological processes, cellular components, and molecular functions. Of note, as highlighted in Fig. 3A, the pathways involved in iron homeostasis and uptake were significantly enriched. Iron uptake occurs mainly through two primary routes in bacteria (*28*). On one hand, the bacteria are able to import either ferric or ferrous cation through iron-chelating siderophore, and, on the other hand, the free ferrous ions can diffuse into periplasm of bacteria via porins, where they are subsequently transported into the cytoplasm by a panel of cytoplasmic proteins. Considering that iron is vital for bacterial physiology, it is possible that the candidate flavonoids resensitize the bacteria to colistin by disrupting their iron homeostasis. In this regard, we profiled the expression of genes associated with iron uptake and found that nearly all selected genes were repressed in response to 7,8-DHF (Fig. 3B and fig. S4). To test whether the flavonoid-mediated iron disruption was responsible for the observed synergy, we applied the colistin in combination with candidate flavonoids on the strain defective in iron transport (*tonB*-deficient and *feoB*-deficient) as well as their isogenic parental strain. The results indicated that the deficiency in *tonB*, the major transmembrane importer of ferric cation, abolished the synergism of MYR and LUT. As to the 7,8-DHF, knockout of *tonB* and *feoB* also significantly impair its synergism with colistin, but to a lesser extent (Fig. 3C).

Then, we investigated the mechanistic insights into iron dysregulation mediated by flavonoids. The intracellular iron contents of bacteria were measured, and sharp decreases in total iron were observed after treatment with 7,8-DHF, MYR, and LUT (Fig. 3D). Note that the decline in ferric iron accounted for the majority of intracellular iron loss comparing with ferrous iron, and the iron was more in the ferrous form than in the ferric form (Fig. 3E). This is interesting because iron normally occurs in its biologically relevant ferric form because the ferrous ion is unstable under aerobic conditions (*29*). The excessive ferrous iron binds with Fur (ferric uptake regulator) as a cofactor, which thereafter represses iron acquisition via gene regulation (*30*). Thus, we assumed that the application of 7,8-DHF, MYR, and LUT decreased pool of accessible ferric iron by converting iron to ferrous form and subsequent blocking iron uptake via Fur regulon. To test this, the free ferric iron was incubated with 7,8-DHF, MYR, and LUT, and the majority of them were transformed into ferrous form, probably due to the reducibility of the flavonoids (Fig. 3F). As a comparison, the flavonoids without synergy (non–catechol-type) showed negligible ferrous iron conversion. In addition, the isothermal titration calorimetry (ITC) tests were performed to determine the interaction between the ferric iron with three candidate flavonoids. The result demonstrated that equilibrium dissociation constant (K_d) values between ferric iron and candidate flavonoids are 1.231×10^{-6} M

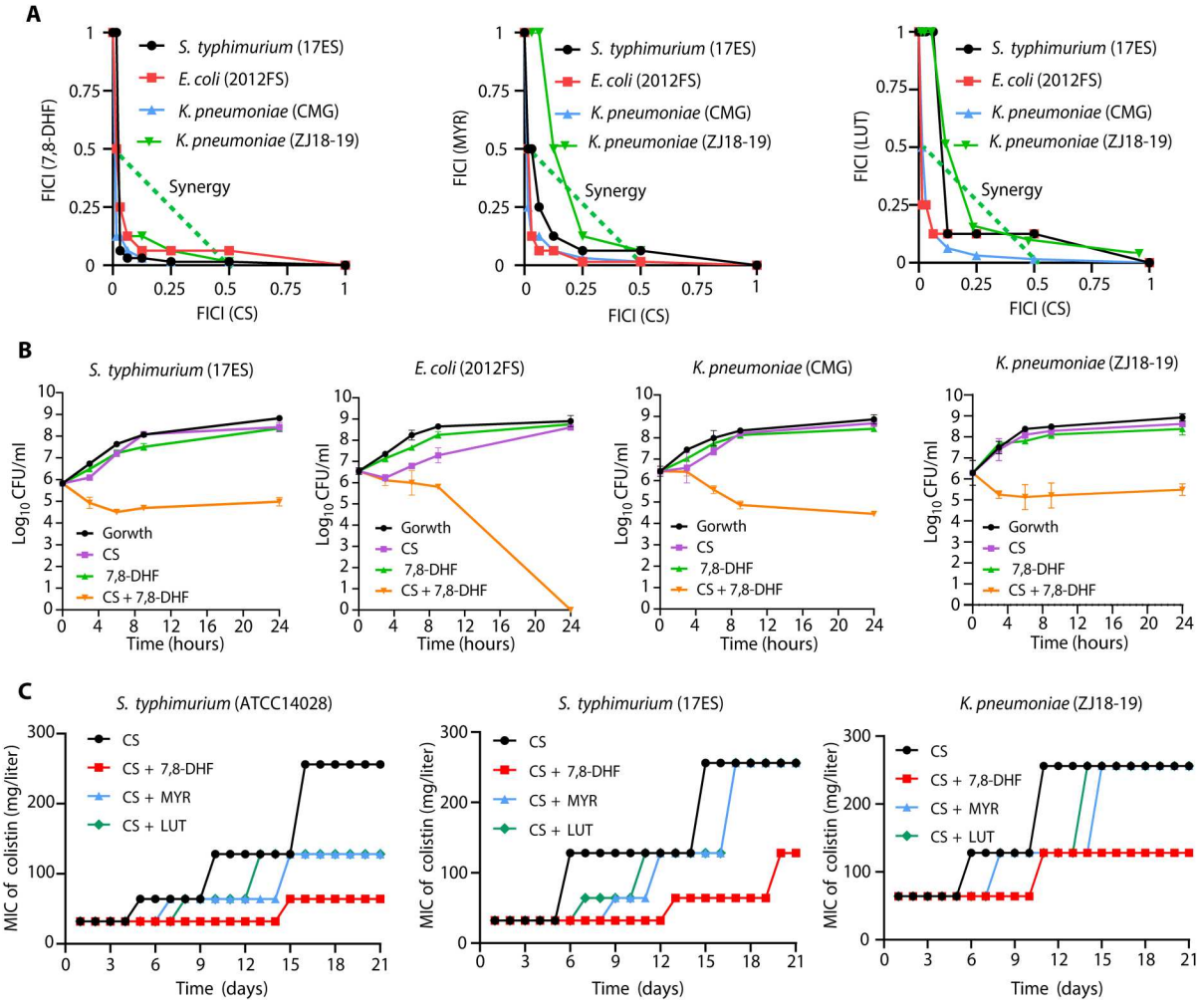

Fig. 2. Candidate flavonoids restore the colistin activity against colistin-resistant bacteria and reduce the emergence of resistance. (**A**) Isobolograms of the combination of colistin (CS) and 7,8-DHF against different colistin-resistant isolates (17ES, *mcr*-positive *S. typhimurium*; 2012FS, *mcr*-positive *E. coli*; CMG, *mcr*-positive *K. pneumoniae*; ZJ18-19, *mgrB*-disrupted *K. pneumoniae*). (**B**) Time-dependent killing of colistin-resistant isolates by the combination of colistin and 7,8-DHF. (**C**) The addition of candidate flavonoids prevented the development of colistin resistance in vitro.

(7,8-DHF), 4.064×10^{-7} M (MYR), and 8.866×10^{-7} M (LUT), suggesting that they had high affinities for ferric ion to convert them into ferrous form (fig. S5). To further test whether the reduced availability of ferric iron was responsible for the resensitization of bacteria to colistin, the potentiation of candidate flavonoids to colistin was determined with or without exogenous ferric iron. Consistently, exogenous addition of ferric iron abolished the synergistic interaction in a dose-dependent manner (Fig. 3G). Together, these findings indicated that 7,8-DHF, MYR, and LUT potentiate colistin efficacy through disruption of bacterial iron homeostasis. However, 7,8-DHF might have additional modes of action to restore colistin sensitivity besides iron modulation.

Candidate flavonoids facilitate colistin binding through iron dysregulation

With the confirmed role of iron in flavonoid-mediated synergism, we next sought to depict what modulated colistin sensitivity in response to iron dysregulation. The Kyoto Encyclopedia of Genes and Genomes (KEGG) enrichment analysis was performed on the basis of our transcriptomic data. As shown in Fig. 4A, eight pathways were enriched, including two-component systems (TCSs), which had the highest number of DEGs among the pathways. Bacterial TCSs are the systems of signal transduction that encompass a response regulator that modulates the response by regulating gene expression and its cognate sensor histidine kinase that detects a specific signal (*31*). Metal ions are among the external signals that can be sensed by TCSs, where *pmrA*/*pmrB* was previously reported to sense iron and modulate the colistin sensitivity by lipopolysaccharide (LPS) modifications (Fig. 4B) (*19*, *32*, *33*). Hence, it was plausible that *pmrA*/*pmrB* responded to the iron dysregulation and induced LPS remodeling.

To test this hypothesis, the promoters of two genes that modulate LPS modification under *pmrA*/*pmrB* control, namely, *arnT* and *eptA*, were fused with a luciferase (*lux*) to construct the transcriptional reporters as indicators for *pmrA*/*pmrB* activation. Consistent with our hypothesis, the promoter activity of selected genes was stimulated by colistin alone but markedly reduced by the treatment of colistin in combination 7,8-DHF, MYR, and LUT, suggesting an

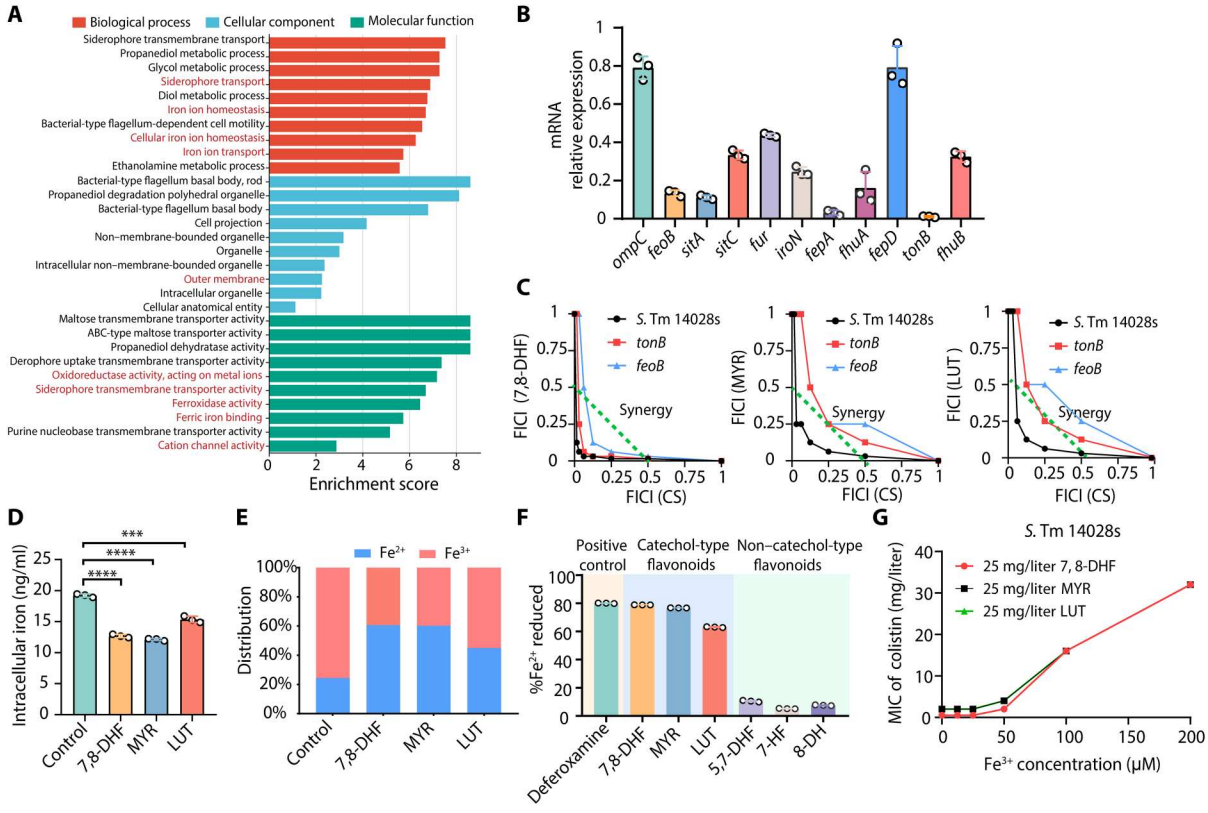

Fig. 3. Candidate flavonoids target bacterial iron homeostasis to potentiate colistin activity. (**A**) Gene Ontology (GO) annotation analysis of the DEGs in bacteria treated by the combination of colistin and 7,8-DHF. ABC, ATP-binding cassette. (**B**) Expression level of genes responsible for bacterial iron acquisition. (**C**) Isobolograms of the combination of colistin and candidate flavonoids against *tonB*-/*feoB*-deficient mutants. (**D**) Candidate flavonoids reduced bacterial intracellular iron contents. (**E**) Candidate flavonoids rapidly converted intracellular iron from ferric form to ferrous form. (**F**) Catechol-type flavonoids strongly reduced iron to the ferrous form. (**G**) The addition of exogenous ferric iron abolished the synergy between colistin with candidate flavonoids.

inactivation of *pmrA*/*pmrB* by the 7,8-DHF, MYR, and LUT (Fig. 4C). To explore how 7,8-DHF, MYR, and LUT regulated the *pmrA*/*pmrB* inactivation, a Phos-tag assay was performed to investigate the impact of these flavonoids on *pmrA* phosphorylation. The utilization of 7,8-DHF, MYR, and LUT with colistin reduced the phosphorylation of *pmrA* in a dose-dependent fashion (Fig. 4D).

To further validate the role of *pmrA*/*pmrB* in flavonoid-mediated synergy, we determined the activity of the colistin-flavonoid combination in mutants with defects in *pmrA* and *pmrB*. For MYR and LUT, deletion of *pmrA* and *pmrB* diminished their synergistic interaction with colistin. As for 7,8-DHF, the synergy was only dampened but not abolished in the strains lack of iron-responsive TCSs. This was consistent with our observations in the section above, indicating that 7,8-DHF uses other potentiation mechanisms in concert with *pmrA*/*B* inactivation (Fig. 4E and fig. S6).

As mentioned above, *arnT* and *eptA* respond to *pmrA*/*pmrB* to catalyze modification of lipid A with phosphoethanolamine (pEtN), allowing the bacterial membrane more positively charged to protect against cationic peptides. To elucidate whether TCS inactivation enhanced colistin binding by preventing LPS modification, the binding affinity of colistin on bacterial membrane in the presence or absence of candidate flavonoids was determined using an enzyme-linked immunosorbent assay (ELISA) kit. The results demonstrated that the addition of 7,8-DHF, MYR, and LUT substantially promoted the binding of colistin to bacteria, which could account for improved efficacy of colistin in combination with three candidate flavonoids (Fig. 4F). Although the bactericidal mechanism of colistin is still not fully understood, it is believed that the collapse of bacterial membrane and the generation of ROS are associated with colistin-caused bacterial death (*34*). Using dyes for detection of membrane permeability and intracellular ROS, we found that the significantly increased membrane permeability and ROS production were observed in bacteria treated by colistin in combination with candidate flavonoids but not in the bacteria treated by colistin alone, which partially explained the mode of action of enhanced bactericidal effects (Fig. 4, G and H). In summary, our results show that 7,8-DHF, MYR, and LUT cause iron dysregulation, which inactivates the TCS of *pmrA*/*pmrB* and suppresses LPS modification, leading to enhanced colistin binding on the bacterial membrane. As a consequence, membrane disruption and ROS production were promoted in response to excessive ferrous iron and colistin, ultimately leading to bacterial cell death.

Candidate flavonoids enhance colistin efficacy in vivo

With the observation of the promising synergism between three flavonoids with colistin in vitro, it is essential to assess the efficacy of these combinatorial therapies in vivo. To this end, 7,8-DHF was selected as a representative flavonoid to be combined with colistin in a mouse salmonellosis model. The procedure of the animal trial was schematically illustrated as Fig. 5A. Throughout the experiment

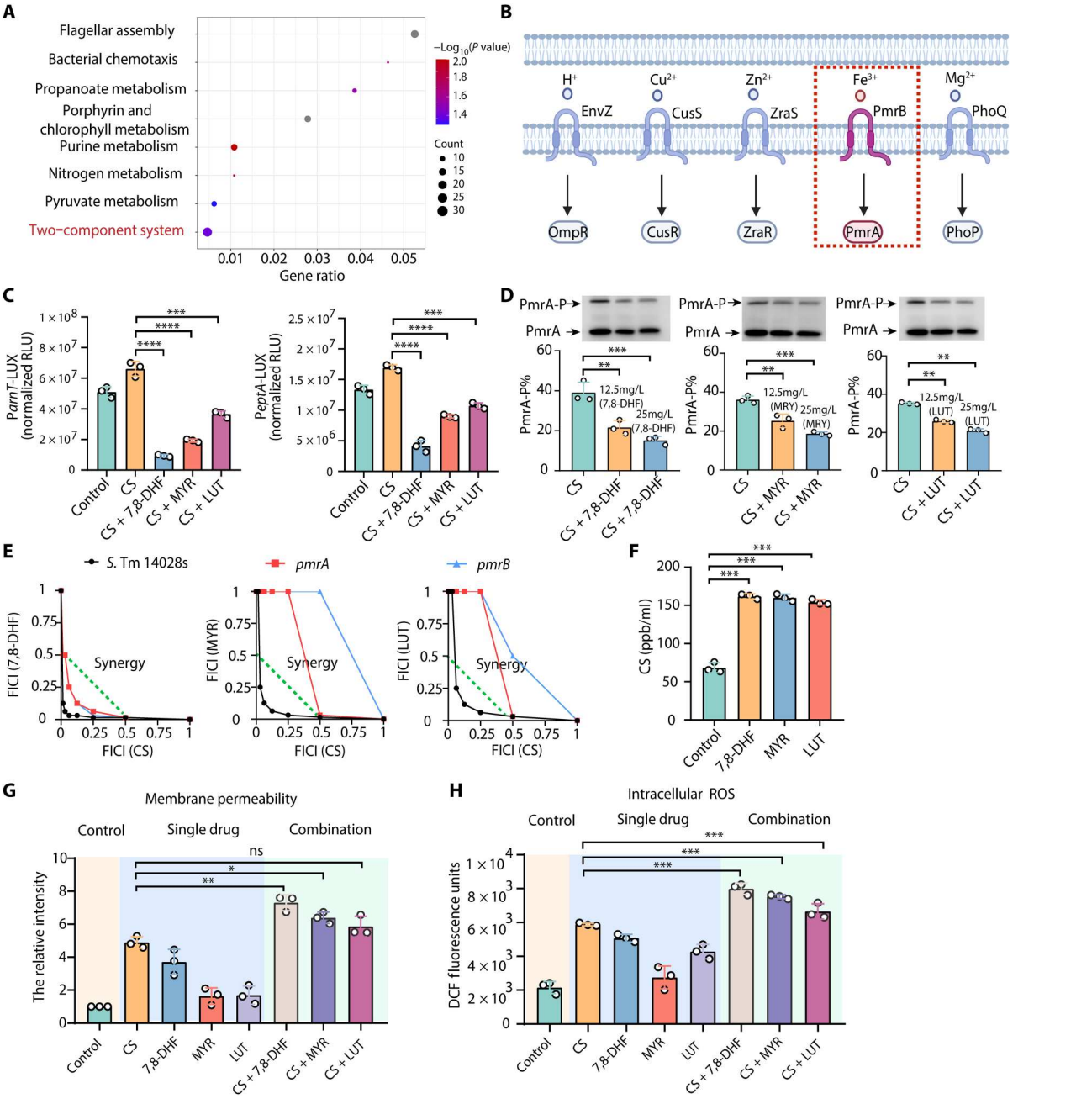

Fig. 4. Candidate flavonoids dysregulate bacterial iron status to inactivate *pmrA* phosphorylation. (**A**) Pathway enrichment of DEGs in bacteria treated by the combination of colistin and 7,8-DHF. (**B**) Scheme of bacterial ion-responsive two-component systems (TCSs). (**C**) Transcriptional reporter assay demonstrated that the two genes modulating LPS modification under *pmrA*/*pmrB* control were suppressed by candidate flavonoids. (**D**) Candidate flavonoids reduced the phosphorylation of regulator PmrA. (**E**) Synergism between colistin and candidate flavonoids was abolished in the mutants lacking *pmrA* and *pmrB*. (**F**) Candidate flavonoids enhanced colistin binding on bacterial membrane by modulating the *pmrA*/*pmrB* TCS. ppb, parts per billion. (**G**) Membrane permeability of bacterial cells after treatment with colistin with or without 7,8-DHF, MYR, and LUT. ns, not significant. (**H**) Accumulation of ROS in bacterial cells after treatment with colistin with or without 7,8-DHF, MYR, and LUT. DCF, Dichlorofluorescein.

(Fig. 5, B to E), animals receiving 7,8-DHF–colistin dual therapy demonstrated significantly increased survival (87.5%), which was superior to single-compound therapy using colistin (25%) or 7,8-DHF (12.5%). Furthermore, the bacteria burdens in feces, liver, and spleen were compared. The results indicated that the combinatorial therapy effectively eradicated the *Salmonella* in the liver and spleen in comparison to using colistin alone. In the fecal samples of the animals treated with 7,8-DHF and colistin, a reduction was observed, although the different is not statistically significant. Our above results demonstrated that the flavonoid can also restore colistin efficacy in vivo, highlighting the promising potentials of these

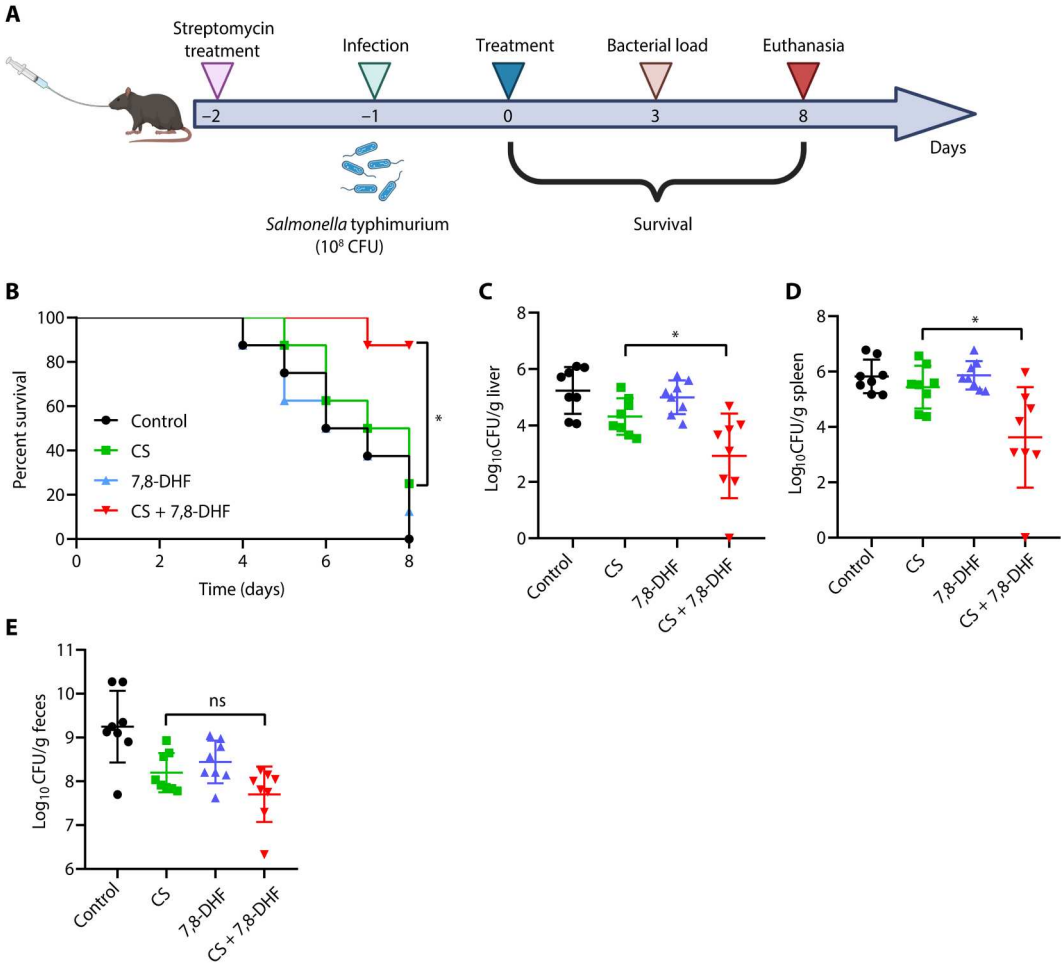

Fig. 5. Candidate flavonoids enhance colistin efficacy in vivo. (**A**) Schematic illustration of experimental protocol for the animal trial. (**B**) Survival curve of infected mice with different treatments. (**C**) Bacterial load in the liver of infected mice with different treatments. (**D**) Bacterial load in the spleen of infected mice with different treatments. (**E**) Bacterial load in feces of infected mice with different treatments.

flavonoids as antibiotic adjuvants to combat clinically important pathogens.

DISCUSSION

The development of new antibiotics has lamentably scaled down since the golden era of antimicrobials discovery, which was pioneered by the Waksman platform (*35*). Thus, alternative approaches are urgently needed to compensate the insufficiency in effective antibiotics for clinical antibiotic therapy. Among these approaches, antibiotic adjuvants that restore or enhance the existing antibiotic efficacy have been deemed as a feasible solution (*36*). In this regard, previous studies have made extensive efforts in uncovering the compounds with properties to potentiate the antibiotics of different classes (*14*, *37*, *38*). The majority of these studies used standard procedures involving rich medium, where bacteria enjoy the optimal growth due to adequate nutrients and stable biochemical conditions. However, this widely applied standard medium generally does not mimic the host conditions and cannot reflect outcomes that may occur in hosts (*39*). For instance, Ersoy and colleagues found that certain conditions in host site were able to considerably alter the bacterial response to antibiotics. Incubation in the microenvironment that simulates macrophage was readily to confer the high-level polymyxin resistance to *S. Typhimurium*. It is also evidenced by recent clinical trials, as the majority of the patients failed to respond to colistin intervention (*17*, *18*, *20*). These data demonstrated the heterogeneity and plasticity of antibiotic resistance of bacteria within hosts, which may explain the treatment failure of antibiotics at routinely used doses (*7*). In view of the limitations of the rich medium–based methods, screening for ex vivo/in vivo signals would be more closely elucidate possible potentiation activity of candidate compounds in hosts (*26*). Therefore, in the current study, we probed the synergism between colistin and our chemical collection in a medium mimicking phagosome of eukaryotic cells, where many intracellular pathogens replicate (*40*). In such conditions, bacteria are known to be more resistant to several antibiotics, including colistin, due to exposure in a mildly acidic microenvironment (*26*, *41*, *42*). In our screening, we also observed that the selected flavonoids exhibited better synergy with colistin in LPM relative to in standard MH broth. This indicated that these candidates were expected to more actively potentiate antibiotic efficacy in the niches where the pathogens reside. Therefore, although the

screening method established in this study had its limits in perfectly recapitulating the in vivo conditions, it still provided a valuable tool to select bioactive compounds under simulated conditions and possibly predict their functional activity in hosts.

Phytochemicals are promising sources of bioactive molecules with health-promoting properties, but their role in combating bacterial infections has been long neglected (*43*, *44*). In this study, we screened 37 phytochemicals to identify candidates that could serve as adjuvants to colistin. These phytochemicals interacted differently with colistin, and only a handful of them were able to restore colistin efficacy in the phagosome-mimicking environment. This was consistent with previous studies, which showed that the activities of phytochemicals against bacteria were variable, implying the essential role of side-chain modification for their biochemical/biophysical properties (*45*, *46*). A good example was the investigation by Song *et al.* (*44*), which showed that prenylation at the phenolic skeleton of flavonoids was a prerequisite for their activity on bacteria. In our case, the SAR analysis also showed that the catechol moieties of the flavonoids were responsible for the observed synergism. Our latter experiments demonstrated that the catechol modification endowed the 7,8-DHF, MYR, and LUT with ability to regulate bacterial iron and associated responses. In a prior work, dephostatin, a protein tyrosine phosphatase inhibitor, was found to restore colistin activity against Gram-negative bacteria via silencing TCS *pmrA*/*pmrB* (*47*). Although the mode of action was not clearly elucidated in this study, we assumed that the dephostatin resensitized the bacteria to colistin in a similar way, because this compound also has catechol moieties and inhibits activation of *pmrA*/*pmrB*. There is likely a vast but unrecognized collection of potential colistin adjuvants among natural products, where the catechol moieties are widely found. However, their antimicrobial activity may be also limited by other characteristics, such as membrane permeability.

Iron acts as a critical component to all living organisms (*48*). Apart from being a nutrient for bacterial growth, iron is also versatile in participating in numerous biological processes such as respiration, tricarboxylic acid cycle, oxygen transport, and signal transduction (*49*–*51*). Given that excessive free ferrous irons are known to generate cytotoxic radicals via Fenton reaction, the uptake, utilization, storage, and efflux of iron are tightly controlled in bacteria to avoid lipid or protein damage (*52*). For homeostatic control of iron, bacteria evolve to sense cellular iron status through iron-sulfur clusters or heme as a proxy (*53*, *54*) and then fine-tune the amounts and forms of free irons by mechanisms like production of iron-sequestering ferritin (*55*). In light of the importance of iron homeostasis, bacterial iron metabolism is thought to be an ideal target for the development of antibacterial agents and adjuvants. However, only a few studies had explored the ability of substances to disrupt bacterial iron for therapeutic purpose. One prior attempt was conducted by Goss and colleagues (*56*), and the metal gallium was found to perturb bacterial iron homeostasis by substituting iron from key enzymes. The application of gallium exhibited synergistic interaction with colistin and piperacillin/tazobactam, substantially promoting the bacterial clearance in a time-dependent manner.

In our study, we found that the three natural flavonoids—7,8-DHF, MYR, and LUT—also target bacterial iron homeostasis to potentiate colistin efficacy, but in a different mechanism comparing with gallium. 7,8-DHF, MYR, and LUT actively reprogrammed the intracellular labile iron pool, in which the ferric irons were largely reduced to ferrous form. This change in the iron form of bacteria led to multifaceted cellular responses that collectively defined the synergistic interaction between flavonoids and colistin (Fig. 6). First, the excess of ferrous iron activated the regulator Fur, which consequently resulted in a prominent downturn of ferric iron uptake (*57*). The ferric iron deficiency then paralyzed the corresponding signaling transductions. *PmrA*/*pmrB* not only is an important component in the iron signaling pathways but also governs the lipid A modifications on bacterial membrane (*42*). The flavonoid-mediated iron deficiency prevented *pmrA* from being phosphorylated into active form, suppressing *arnT* and *eptA* at transcriptional level. As a result, the colistin can better target the lipid A in the absence of positively charged molecules like pEtN. The accumulative colistin binding damaged the bacterial membrane while promoting the generation of lethal ROS via disruption of electronic transport chain (*58*, *59*). This bactericidal action of colistin can be augmented by the flavonoid-mediated iron manipulation, as most intracellular irons were transformed to the ferrous form to facilitate the buildup of ROS via Fenton chemistry as additive or synergistic reaction. This explains the rationale behind the observation that 7,8-DHF, MYR, and LUT increased the intracellular ROS either used alone or in combination with colistin.

The accumulation of ferrous iron and ROS are the hallmarks of cell ferroptosis (*60*). Although the concept of ferroptosis is more well explicated in mammalian cells, recent studies elucidated the occurrence of ferroptotic damages in bacterial cells in response to defined conditions or stresses (*61*, *62*). Inspired by such observations, there have been developments of strategies to eradicate bacteria by inducing ferroptosis-like death in bacterial cells (*63*). In light of the ability of 7,8-DHF, MYR, and LUT to promote the accumulation of ferrous iron and ROS in bacteria, these natural flavonoids are also of great potential to mitigate infection as bacteria-specific ferroptosis–like death inducers. In addition to iron, the homeostasis of other intracellular metals has also been shown to affect bacterial responses to antibiotics. For instance, studies have demonstrated that agents with ionophore properties can enhance the activity of a range of antibiotics against MDR bacteria by disrupting intracellular zinc homeostasis (*23*, *64*, *65*). These investigations highlight the potential of targeting bacterial metal homeostasis as a strategy for developing new antimicrobial regimens and underscore the importance of further research in this area.

Although we have elucidated the mechanism of 7,8-DHF, MYR, and LUT, 7,8-DHF is likely to have additional modes of action to potentiate colistin activity besides iron manipulation. Comparing with MYR and LUT, 7,8-DHF still synergized with colistin in mutant strains lacking functions in iron transporting or iron responding. Thus, further studies are needed to depict what else contributes to the potentiation to colistin by 7,8-DHF besides modulating bacterial iron form. A more in-depth understanding of the better activity of 7,8-DHF than the other two flavonoids could also benefit the structural optimization of flavonoid-based compounds as antibiotic adjuvants.

In conclusion, three catechol-type flavonoids—7,8-DHF, MYR, and LUT—were identified as adjuvants to colistin in a screening based on host-mimicking condition. These three flavonoids are able to disrupt bacterial iron homeostasis, thereby dysregulating the iron signaling to enhance colistin binding and ROS production. This work shed the light on the potential of untapped phytochemicals to combat bacterial infections and presented flavonoid-colistin

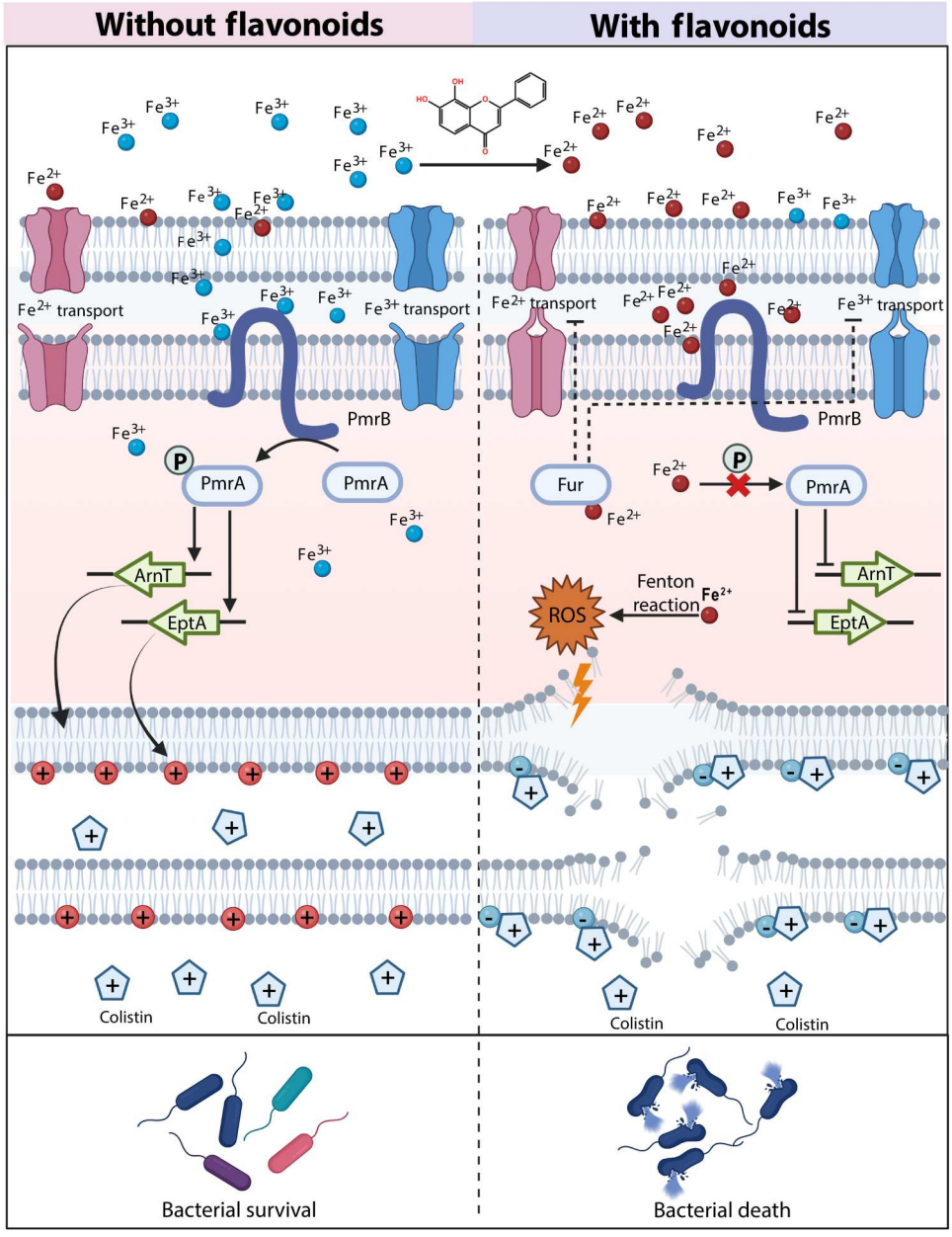

Fig. 6. Mechanistic insight into synergistic interaction between colistin and candidate flavonoids.

combination as a viable treatment choice to eradicate Gram-negative pathogens from the host.

MATERIALS AND METHODS

Bacterial strains and cultivation

The bacterial strains used in this study are listed in table S1. All experiments with *Salmonella* were performed with *S.* Tm str. 14028s or its isogenic derivatives unless otherwise noted. Routine propagation of bacteria was conducted in Luria-Bertani (LB) medium. The subculture was 1:100 diluted and grown in host-mimicking medium [LPM, 5 mM KCl, 7.5 mM $(NH4)_2SO_4$, 0.5 mM K_2SO_4, 80 mM MES (pH 5.8), 0.1% casamino acids, 0.3% (v/v) glycerol, 24 μM $MgCl_2$, and 337 μM PO_4^{3-}]. The antimicrobial susceptibilities of all tested strains were determined by LPM in pH 5.8 (*26*).

Genetic manipulation of strains

All plasmids and primers used in this study were listed in tables S3 and S4. All plasmids were extracted using the TIANprep Mini Plasmid Kit (Tiangen, China). The *pmrA*, *pmrB*, *feoB*, and *tonB* genes in *S.* Tm str. 14028s were knocked out using a λRed recombination system to generate corresponding mutant strains (*66*). The pUC19 plasmid was used as the vector backbone to create a bioluminescent reporter system, where the promoter of selected genes (*arnT* and *eptA*) and LuxCDABE were fused to form the plasmids P_{arnT}-Lux and P_{eptA}-Lux, respectively. Using the same method, the

pmrA fragment was fused with a hemagglutinin (HA) tag and integrated into the vector of pBAD24 to obtain the plasmid pBAD24::*pmrA*-HA.

Primary screening of colistin adjuvants

A total of 37 phytochemicals from our laboratory collection were subjected to primary screening using a host-mimicking medium LPM. Overnight bacterial culture was suspended in LPM and dispensed in a microtiter plate, yielding a final load of 5×10^3 cells per well. Colistin and each phytochemical were supplemented at the indicated concentration; then, the plates were incubated aerobically at 37°C with shacking at 50 rpm for 18 hours, and the growth (OD_{600nm}) was recorded using a microtiter plate reader (PerkinElmer, USA). The OD_{600nm} of bacteria in the presence of colistin, phytochemicals, or the combinations relative to that of no-drug control was presented as W_X, W_Y, and W_{XY}, respectively. After the incubation, the interaction between colistin and each phytochemical was assessed using a previously published method (*27*). Briefly, the $\tilde{\varepsilon}$ value was introduced to define the interaction between colistin and the phytochemicals used. The $\tilde{\varepsilon}$ value was calculated as $(W_{XY} - W_X W_Y)/(\tilde{W}_{XY} - W_X W_Y|)$, where $\tilde{W}_{XY}$ was equal to min $[W_X, W_Y]$ for $W_{XY} > W_X W_Y$ and 0 otherwise. If $\tilde{W}_{XY}$ was greater than min $[W_X, W_Y]$, then $\tilde{\varepsilon}$ was equal to $\{(W_{XY} - \min [W_X, W_Y])/(1 - \min [W_X, W_Y])\} + 1$. When $\tilde{\varepsilon}$ falls within the range of −1 to −0.5, the interaction was defined as synergism; otherwise, it was classified as additive or antagonistic.

Antimicrobial susceptibility testing and checkerboard assay

The MIC assay was performed to determine the antimicrobial susceptibility according to the standard protocol. The results were interpreted on the basis of the guidelines of the Clinical and Laboratory Standards Institute. Briefly, both drugs were twofold diluted in medium and mixed with an equal volume of bacterial suspensions [10^6 colony-forming units (CFU)/ml] in microtiter plate. After incubation at 37°C for 18 hours, the MIC values were defined as the lowest concentrations of antibiotics with no visible growth of bacteria. For better understanding the synergy between colistin and selected phytochemicals, the checkerboard assay was conducted to determine the FICI as described previously with minor modifications (*67*). In brief, 100 μl of LPM broth was first dispensed to each well in a microtiter plate with serial diluted colistin and selected phytochemicals. Subsequently, 5×10^5 CFU/ml of bacteria was inoculated in the same plate and incubated at 37°C for 18 hours. The OD_{600nm} was determined using a microtiter plate reader (PerkinElmer, USA). The FICI was calculated by the formula as follows: FICI = (MIC_A combination/MIC_A alone) + (MIC_B combination/MIC_B alone). FICI values of ≤0.5, 0.5 to 2, and > 2 were defined as synergism, indifference, and antagonism, respectively (*68*).

Time-dependent killing assay

The bacteria were cultured to exponential phase and then diluted in LPM to ~10^6 CFU/ml, which were subsequently treated with subinhibitory concentrations of colistin, the selected flavonoids (25 mg/liter), or their combination. At time points 0, 3, 6, 9, and 24 hours, a 100-μl aliquot of each treatment was removed, diluted, and plated to determine bacterial survivors (*67*).

Resistance development study

Overnight cultures of *S.* Tm str. 14028s and colistin-resistant isolates (17ES and ZJ18-19) were harvested in fresh LB medium. The bacterial cultures were then incubated at 37°C in LPM containing sublethal colistin with or without selected flavonoids under continuous shaking at 200 rpm for 24 hours. The cultures were serially passaged for 21 days, during which the MIC of evolved bacterial subpopulation of each strain was monitored (*47*).

RNA-seq and transcriptomic analysis

The *S.* Tm str. 14028s was grown in LPM to the exponential phase and treated with 7,8-DHF and colistin for 4 hours. The bacterial cells were then washed three times, and the total RNA of each sample was extracted using the OMEGA Total RNA Kit I (Omega, China). The RNA-seq library was constructed with the Illumina TruSeq RNA sample Prep Kit v2 (Illumina, USA) according to a previous protocol (*69*). In brief, mRNA was sheared into lengths of 200 to 300 base pairs; thereafter, the first and second strand complementary DNAs (cDNAs) were synthesized. The short cDNA fragments were purified and tailed with single A (adenine) addition. Adapters were ligated to the A-tailed cDNA fragments. For the transcriptomic analysis, short sequences (reads) were mapped to the reference sequence (www.ncbi.nlm.nih.gov/nuccore/NC_003197) using FANse2 software, and the number of reads of each gene was used to estimate the level of gene expressions. The DEGs were annotated by $Q \leq 0.01$ and absolute log fold change ≥ 2. The GO enrichment analysis of DEGs was performed by ClueGO in Cytoscape (*70*).

RNA isolation and RT-qPCR

The total RNA of treated bacterial cells was extracted using the OMEGA Total RNA Kit I (Omega, China). Reverse transcription was conducted with 1 μg of total RNA using the GoldenstarRT cDNA Synthesis Mix (TsingKe Biotech, China). The reverse transcription quantitative polymerase chain reaction (RT-qPCR) was performed using the SYBR Master Mix (Vazyme, China). The primers used for RT-qPCR were provided in table S4. The gene expressions were presented as relative expression using the $2^{-\Delta\Delta Ct}$ method (Livak method) as elucidated previously (*71*).

Intracellular iron profiling

The bacterial cultures were harvested after coincubation with candidate flavonoids and then were homogenized by sonication. The cell lysates were collected for the determination of intracellular iron content using a previous method with minor modifications (*72*). The Total Iron Colorimetric Assay Kit (E-BC-K139-M, Elabscience, USA) was used to quantify the total iron in bacterial cells, and the Cell Ferrous Iron Colorimetric Assay Kit (E-BC-K881-M, Elabscience, USA) was used to estimate the iron in ferrous form.

Iron reduction assay

To test the ability of candidate flavonoids to interfere iron forms, ferrozine probe was used on the basis of a previous protocol with minor modifications (*73*). The ferric iron ($FeCl_3$) was suspended in LPM to yield a final concentration of 100 μM. Then, 7,8-DHF, MYR, and LUT were incubated in the suspension for 10 min, followed by the supplementation of ferrozine. In addition, 5,7-dihydroxyflavone, 7-hydroxyflavone, and 8-hydroxyflavone were used as negative controls, and deferoxamine was used as a positive

control. Last, the absorption of samples was monitored by microtiter plate reader at OD_{562}, and the ferrous/ferric iron ratio was determined.

Isothermal titration calorimetry

The interactions between ferric ion and candidate flavonoids were determined by ITC (TA Instruments, USA) at 25°C. The respective compounds were dissolved in water. The $FeCl_3$ solution was injected repeatedly 25 times with equilibration intervals of 180 s. The obtained data were processed using the software provided with the instrument to calculate the equilibrium K_d.

Transcriptional reporter assay

Wild-type or mutant *Salmonella* was transformed with the pUC-luxCDABE plasmid fused with promoters of targeted genes. The bacteria were grown in LB to the exponential phase and then transferred into LPM. After incubation of 6 hours, the luminescence and OD_{600nm} were measured. The luminescence [Relative Light Unit (RLU)] was normalized to OD_{600nm}. A concentration of 25 mg/liter of the selected flavonoids was used for all assays.

Phos-tag assay

The phosphorylation of bacterial TCS protein was determined by Phos-tag assay as previously described (*74*). Briefly, 14028/pBAD-*pmrA*-HA was grown in LPM with 0.006% arabinose and selected flavonoids (0, 12.5, and 25 mg/liter). During the exponential phase, cell pellets were washed with ice-cold 10 mM tris-Cl (pH 6.8) buffer and lysed. A total of 200 μl of lysate of each sample was combined with 100 μl of 3× SDS loading buffer and then heated at 95°C for 5 min. After heating, 10 μl of aliquot was loaded onto a Phos-tag gel. Target proteins were separated by electrophoresis at 4°C and then transferred to a polyvinylidene difluoride for immunoblotting. The blots were probed with indicated antibodies, and the protein phosphorylation was quantified with ImageJ.

Colistin binding assay

The binding affinity of colistin to bacterial membrane, after treatment with candidate flavonoids, was assessed using a previous method with minor modifications (*75*). In brief, the bacterial cells were incubated with colistin in the presence or absence of candidate flavonoids at 37°C for 30 min. The cell pellets were then washed three times and resuspended in saline solution. Colistin bound to the bacterial membrane was dissociated by adding 200 μl of glycine-HCl buffer (pH 2.4) for 30 min. Colistin was quantitatively detected using the Colistin ELISA Test Kit EVCOL-02 (Kernel, USA) according to the manufacturer's instructions.

Membrane permeability test

The membrane permeability test was performed on the basis of a previous protocol (*76*). Bacteria were first treated by colistin in the presence or absence of candidate flavonoids at 37°C for 30 min. Then, the fluorescent dye propidium iodide (30 μM) was added to each sample followed by shaking at 100 rpm for 30 min in the dark. The fluorescent signals were measured using the CytExpert Flow Cytometer (Beckman, USA) at an excitation wavelength of 488 nm and an emission wavelength of 630 nm. All tests were performed in triplicate, and the raw data were analyzed using CytExpert 2.0 software (Beckman, USA).

ROS determination by flow cytometry

Intracellular ROS was determined using a microplate reader according to the method previously reported (*37*). An ROS-sensitive dye (DCFH-DA, 10 μM) was added in the growth medium to detect overall intracellular ROS in bacteria challenged by colistin, flavonoids, and their combinations. After incubation for 30 min, the fluorescence intensity was measured with the excitation wavelength at 488 nm and emission wavelength at 525 nm.

Animal trial

Female C57BL/6J mice at 8 weeks of age were orally infected with a lethal dose of *S*. Tm str. 14028s (~10^8 CFU). The infected mice were divided into four groups (n = 8 per group) and received, respectively, (i) phosphate-buffered saline (control), (ii) 7,8-DHF (5 mg/kg), (iii) colistin (5 mg/kg), and (iv) the combination of 7,8-DHF with colistin (5 mg/kg for both) through the intraperitoneal route 1 day after infection. Three days after the treatment, bacterial loads in the liver, spleen, and stool were enumerated, and the survival of mice in each group was monitored throughout the experiment (*47*, *77*, *78*).

Ethic approval

This study was carried out in accordance with the recommendations of the ethical guidelines of South China Agricultural University. All animal experimental protocols were reviewed and approved by the South China Agricultural University Institutional Animal Ethics Committee (2022c057).

Statistical analysis

Results are presented as means ± SD. The statistical analysis was performed using SPSS software (IBM, USA). Unless stated otherwise, the statistical significance of comparison was assessed using the unpaired T test or one-way analysis of variance (ANOVA) (*P < 0.05, **P < 0.01, ***P < 0.001, and ****P < 0.0001).

Supplementary Materials

This PDF file includes:
Figs. S1 to S6
Tables S1 to S4
Legends for supplemental Excel

Other Supplementary Material for this manuscript includes the following:
Supplemental Excel

REFERENCES AND NOTES

1. J. Davies, D. Davies, Origins and evolution of antibiotic resistance. *Microbiol. Mol. Biol. Rev.* **74**, 417–433 (2010).
2. E. D. Brown, G. D. Wright, Antibacterial drug discovery in the resistance era. *Nature* **529**, 336–343 (2016).
3. B. M. Kuehn, Alarming antimicrobial resistance trends emerge globally. *JAMA* **324**, 223 (2020).
4. Y.-Y. Liu, Y. Wang, T. R. Walsh, L.-X. Yi, R. Zhang, J. Spencer, Y. Doi, G. Tian, B. Dong, X. Huang, L.-F. Yu, D. Gu, H. Ren, X. Chen, L. Lv, D. He, H. Zhou, Z. Liang, J.-H. Liu, J. Shen, Emergence of plasmid-mediated colistin resistance mechanism MCR-1 in animals and human beings in China: A microbiological and molecular biological study. *Lancet Infect. Dis.* **16**, 161–168 (2016).
5. J. Sun, C. Chen, C.-Y. Cui, Y. Zhang, X. Liu, Z.-H. Cui, X.-Y. Ma, Y. Feng, L.-X. Fang, X.-L. Lian, R.-M. Zhang, Y.-Z. Tang, K.-X. Zhang, H.-M. Liu, Z.-H. Zhuang, S.-D. Zhou, J.-N. Lv, H. Du, B. Huang, F.-Y. Yu, B. Mathema, B. N. Kreiswirth, X.-P. Liao, L. Chen, Y.-H. Liu, Plasmid-

encoded *tet*(X) genes that confer high-level tigecycline resistance in *Escherichia coli*. *Nat. Microbiol.* **4**, 1457–1464 (2019).

6. K. K. Kumarasamy, M. A. Toleman, T. R. Walsh, J. Bagaria, F. Butt, R. Balakrishnan, U. Chaudhary, M. Doumith, C. G. Giske, S. Irfan, P. Krishnan, A. V. Kumar, S. Maharjan, S. Mushtaq, T. Noorie, D. L. Paterson, A. Pearson, C. Perry, R. Pike, B. Rao, U. Ray, J. B. Sarma, M. Sharma, E. Sheridan, M. A. Thirunarayan, J. Turton, S. Upadhyay, M. Warner, W. Welfare, D. M. Livermore, N. Woodford, Emergence of a new antibiotic resistance mechanism in India, Pakistan, and the UK: A molecular, biological, and epidemiological study. *Lancet Infect. Dis.* **10**, 597–602 (2010).
7. J. Z. Kubicek-Sutherland, D. M. Heithoff, S. C. Ersoy, W. R. Shimp, J. K. House, J. D. Marth, J. W. Smith, M. J. Mahan, Host-dependent induction of transient antibiotic resistance: A prelude to treatment failure. *eBioMedicine* **2**, 1169–1178 (2015).
8. L. L. Ling, T. Schneider, A. J. Peoples, A. L. Spoering, I. Engels, B. P. Conlon, A. Mueller, T. F. Schäberle, D. E. Hughes, S. Epstein, M. Jones, L. Lazarides, V. A. Steadman, D. R. Cohen, C. R. Felix, K. A. Fetterman, W. P. Millett, A. G. Nitti, A. M. Zullo, C. Chen, K. Lewis, A new antibiotic kills pathogens without detectable resistance. *Nature* **517**, 455–459 (2015).
9. V. Lázár, O. Snitser, D. Barkan, R. Kishony, Antibiotic combinations reduce *Staphylococcus aureus* clearance. *Nature* **610**, 540–546 (2022).
10. Y. Liu, Z. Tong, J. Shi, R. Li, M. Upton, Z. Wang, Drug repurposing for next-generation combination therapies against multidrug-resistant bacteria. *Theranostics* **11**, 4910–4928 (2021).
11. Y. Imai, K. J. Meyer, A. Iinishi, Q. Favre-Godal, R. Green, S. Manuse, M. Caboni, M. Mori, S. Niles, M. Ghiglieri, C. Honrao, X. Ma, J. J. Guo, A. Makriyannis, L. Linares-Otoya, N. Böhringer, Z. G. Wuisan, H. Kaur, R. Wu, A. Mateus, A. Typas, M. M. Savitski, J. L. Espinoza, A. O'Rourke, K. E. Nelson, S. Hiller, N. Noinaj, T. F. Schäberle, A. D'Onofrio, K. Lewis, A new antibiotic selectively kills Gram-negative pathogens. *Nature* **576**, 459–464 (2019).
12. M. Tyers, G. D. Wright, Drug combinations: A strategy to extend the life of antibiotics in the 21st century. *Nat. Rev. Microbiol.* **17**, 141–155 (2019).
13. C. Reading, M. Cole, Clavulanic acid: A beta-lactamase-inhibiting beta-lactam from *Streptomyces clavuligerus*. *Antimicrob. Agents Chemother.* **11**, 852–857 (1977).
14. M. Song, Y. Liu, X. Huang, S. Ding, Y. Wang, J. Shen, K. Zhu, A broad-spectrum antibiotic adjuvant reverses multidrug-resistant Gram-negative pathogens. *Nat. Microbiol.* **5**, 1040–1050 (2020).
15. S. Biswas, J.-M. Brunel, J.-C. Dubus, M. Reynaud-Gaubert, J.-M. Rolain, Colistin: An update on the antibiotic of the 21st century. *Expert Rev. Anti Infect. Ther.* **10**, 917–934 (2012).
16. D. Yahav, L. Farbman, L. Leibovici, M. Paul, Colistin: New lessons on an old antibiotic. *Clin. Microbiol. Infect.* **18**, 18–29 (2012).
17. M. E. Falagas, P. I. Rafailidis, E. Ioannidou, V. G. Alexiou, D. K. Matthaiou, D. E. Karageorgopoulos, A. Kapaskelis, D. Nikita, A. Michalopoulos, Colistin therapy for microbiologically documented multidrug-resistant Gram-negative bacterial infections: A retrospective cohort study of 258 patients. *Int. J. Antimicrob. Agents* **35**, 194–199 (2010).
18. M. Paul, G. L. Daikos, E. Durante-Mangoni, D. Yahav, Y. Carmeli, Y. D. Benattar, A. Skiada, R. Andini, N. Eliakim-Raz, A. Nutman, O. Zusman, A. Antoniadou, P. C. Pafundi, A. Adler, Y. Dickstein, I. Pavleas, R. Zampino, V. Daitch, R. Bitterman, H. Zayyad, F. Koppel, I. Levi, T. Babich, L. E. Friberg, J. W. Mouton, U. Theuretzbacher, L. Leibovici, Colistin alone versus colistin plus meropenem for treatment of severe infections caused by carbapenem-resistant Gram-negative bacteria: An open-label, randomised controlled trial. *Lancet Infect. Dis.* **18**, 391–400 (2018).
19. A. Sabnis, K. L. H. Hagart, A. Klöckner, M. Becce, L. E. Evans, R. C. D. Furniss, D. A. I. Mavridou, R. Murphy, M. M. Stevens, J. C. Davies, G. J. Larrouy-Maumus, T. B. Clarke, A. M. Edwards, Colistin kills bacteria by targeting lipopolysaccharide in the cytoplasmic membrane. *eLife* **10**, e65836 (2021).
20. P. K. Linden, S. Kusne, K. Coley, P. Fontes, D. J. Kramer, D. Paterson, Use of parenteral colistin for the treatment of serious infection due to antimicrobial-resistant *Pseudomonas aeruginosa*. *Clin. Infect. Dis.* **37**, e154–e160 (2003).
21. M. J. Satlin, J. S. Lewis II, M. P. Weinstein, J. Patel, R. M. Humphries, G. Kahlmeter, C. G. Giske, J. Turnidge, Clinical and laboratory standards institute and European committee on antimicrobial susceptibility testing position statements on polymyxin B and colistin clinical breakpoints. *Clin. Infect. Dis.* **71**, e523–e529 (2020).
22. Y. Liu, Y. Jia, K. Yang, Z. Tong, J. Shi, R. Li, X. Xiao, W. Ren, R. Hardeland, R. J. Reiter, Z. Wang, Melatonin overcomes MCR-mediated colistin resistance in Gram-negative pathogens. *Theranostics* **10**, 10697–10711 (2020).
23. D. M. P. De Oliveira, L. Bohlmann, T. Conroy, F. E.-C. Jen, A. Everest-Dass, K. A. Hansford, R. Bolisetti, I. M. El-Deeb, B. M. Forde, M.-D. Phan, J. A. Lacey, A. Tan, T. Rivera-Hernandez, S. Brouwer, N. Keller, T. J. Kidd, A. J. Cork, M. J. Bauer, G. M. Cook, M. R. Davies, S. A. Beatson, D. L. Paterson, A. G. McEwan, J. Li, M. A. Schembri, M. A. T. Blaskovich, M. P. Jennings, C. A. McDevitt, M. von Itzstein, M. J. Walker, Repurposing a neurodegenerative disease drug to treat Gram-negative antibiotic-resistant bacterial sepsis. *Sci. Transl. Med.* **12**, eabb3791 (2020).
24. Q. Zhang, R. Wang, M. Wang, C. Liu, M. Koohi-Moghadam, H. Wang, P.-L. Ho, H. Li, H. Sun, Re-sensitization of *mcr* carrying multidrug resistant bacteria to colistin by silver. *Proc. Natl. Acad. Sci. U. S.A.* **119**, e2119417119 (2022).
25. S. C. Ersoy, D. M. Heithoff, L. V. Barnes, G. K. Tripp, J. K. House, J. D. Marth, J. W. Smith, M. J. Mahan, Correcting a fundamental flaw in the paradigm for antimicrobial susceptibility testing. *EBioMedicine* **20**, 173–181 (2017).
26. M. J. Ellis, C. N. Tsai, J. W. Johnson, S. French, W. Elhenawy, S. Porwollik, H. Andrews-Polymenis, M. McClelland, J. Magolan, B. K. Coombes, E. D. Brown, A macrophage-based screen identifies antibacterial compounds selective for intracellular *Salmonella Typhimurium*. *Nat. Commun.* **10**, 197 (2019).
27. A. Zhou, T. M. Kang, J. Yuan, C. Beppler, C. Nguyen, Z. Mao, M. Q. Nguyen, P. Yeh, J. H. Miller, Synergistic interactions of vancomycin with different antibiotics against *Escherichia coli*: Trimethoprim and nitrofurantoin display strong synergies with vancomycin against wild-type *E. coli*. *Antimicrob. Agents Chemother.* **59**, 276–281 (2015).
28. O. Cunrath, J. D. Palmer, An overview of *Salmonella enterica* metal homeostasis pathways during infection. *microLife* **2**, uqab001 (2021).
29. H. Gerken, P. Vuong, K. Soparkar, R. Misra, Roles of the EnvZ/OmpR two-component system and porins in iron acquisition *in Escherichia coli*. *MBio* **11**, e01192-20 (2020).
30. Z. Chen, K. A. Lewis, R. K. Shultzaberger, I. G. Lyakhov, M. Zheng, B. Doan, G. Storz, T. D. Schneider, Discovery of Fur binding site clusters in *Escherichia coli* by information theory models. *Nucleic Acids Res.* **35**, 6762–6777 (2007).
31. M. A. Kohanski, J. J. Collins, Rewiring bacteria, two components at a time. *Cell* **133**, 947–948 (2008).
32. Y. Charretier, S. M. Diene, D. Baud, S. Chatellier, E. Santiago-Allexant, A. v. Belkum, G. Guigon, J. Schrenzel, Colistin heteroresistance and involvement of the PmrAB regulatory system in *Acinetobacter baumannii*. *Antimicrob. Agents Chemother.* **62**, e00788-18 (2018).
33. M. D. Adams, G. C. Nickel, S. Bajaksouzian, H. Lavender, A. R. Murthy, M. R. Jacobs, R. A. Bonomo, Resistance to colistin in *Acinetobacter baumannii* associated with mutations in the PmrAB two-component system. *Antimicrob. Agents Chemother.* **53**, 3628–3634 (2009).
34. M. A. E.-G. El-Sayed Ahmed, L.-L. Zhong, C. Shen, Y. Yang, Y. Doi, G.-B. Tian, Colistin and its role in the era of antibiotic resistance: An extended review (2000–2019). *Emerg. Microbes Infect.* **9**, 868–885 (2020).
35. K. Lewis, Recover the lost art of drug discovery. *Nature* **485**, 439–440 (2012).
36. R. J. Melander, C. Melander, The challenge of overcoming antibiotic resistance: An adjuvant approach? *ACS Infect. Dis.* **3**, 559–563 (2017).
37. Y. Liu, Y. Jia, K. Yang, R. Li, X. Xiao, Z. Wang, Anti-HIV agent azidothymidine decreases Tet(X)-mediated bacterial resistance to tigecycline in *Escherichia coli*. *Commun. Biol.* **3**, 162 (2020).
38. L. Xu, Y. Zhou, S. Niu, Z. Liu, Y. Zou, Y. Yang, H. Feng, D. Liu, X. Niu, X. Deng, Y. Wang, J. Wang, A novel inhibitor of monooxygenase reversed the activity of tetracyclines against *tet*(X3)/*tet* (X4)-positive bacteria. *eBioMedicine* **78**, 103943 (2022).
39. H. Ren, E.-M. Saliu, J. Zentek, F. Goodarzi Boroojeni, W. Vahjen, Screening of host specific lactic acid bacteria active against *Escherichia coli* from massive sample pools with a combination of *in vitro* and *ex vivo* methods. *Front. Microb.* **10**, 2705–2705 (2019).
40. O. Steele-Mortimer, The *Salmonella*-containing vacuole—Moving with the times. *Curr. Opin. Microbiol.* **11**, 38–45 (2008).
41. H. D. Chen, E. A. Groisman, The biology of the PmrA/PmrB two-component system: The major regulator of lipopolysaccharide modifications. *Annu. Rev. Microbiol.* **67**, 83–112 (2013).
42. J. S. Gunn, The *Salmonella* PmrAB regulon: Lipopolysaccharide modifications, antimicrobial peptide resistance and more. *Trends Microbiol.* **16**, 284–290 (2008).
43. D. Carmona-Gutierrez, A. Zimmermann, K. Kainz, F. Pietrocola, G. Chen, S. Maglioni, A. Schiavi, J. Nah, S. Mertel, C. B. Beuschel, F. Castoldi, V. Sica, G. Trausinger, R. Raml, C. Sommer, S. Schroeder, S. J. Hofer, M. A. Bauer, T. Pendl, J. Tadic, C. Dammbrueck, Z. Hu, C. Ruckenstuhl, T. Eisenberg, S. Durand, N. Bossut, F. Aprahamian, M. Abdellatif, S. Sedej, D. P. Enot, H. Wolinski, J. Dengjel, O. Kepp, C. Magnes, F. Sinner, T. R. Pieber, J. Sadoshima, N. Ventura, S. J. Sigrist, G. Kroemer, F. Madeo, The flavonoid 4,4'-dimethoxychalcone promotes autophagy-dependent longevity across species. *Nat. Commun.* **10**, 651 (2019).
44. M. Song, Y. Liu, T. Li, X. Liu, Z. Hao, S. Ding, P. Panichayupakaranant, K. Zhu, J. Shen, Plant natural flavonoids against multidrug resistant pathogens. *Adv. Sci.* **8**, 2100749 (2021).
45. K. Lewis, The science of antibiotic discovery. *Cell* **181**, 29–45 (2020).
46. D. Meier, M. V. Hernández, L. van Geelen, R. Muharini, P. Proksch, J. E. Bandow, R. Kalscheuer, The plant-derived chalcone Xanthoangelol targets the membrane of Gram-positive bacteria. *Bioorg. Med. Chem.* **27**, 115151 (2019).
47. C. N. Tsai, C. R. MacNair, M. P. T. Cao, J. N. Perry, J. Magolan, E. D. Brown, B. K. Coombes, Targeting two-component systems uncovers a small-molecule inhibitor of *Salmonella* virulence. *Cell Chem. Biol.* **27**, 793–805.e7 (2020).

48. E. R. Frawley, F. C. Fang, The ins and outs of bacterial iron metabolism. *Mol. Microbiol.* **93**, 609–616 (2014).
49. K. J. Waldron, J. C. Rutherford, D. Ford, N. J. Robinson, Metalloproteins and metal sensing. *Nature* **460**, 823–830 (2009).
50. B. D'Autréaux, N. P. Tucker, R. Dixon, S. Spiro, A non-haem iron centre in the transcription factor NorR senses nitric oxide. *Nature* **437**, 769–772 (2005).
51. J. E. Karlinsey, I.-S. Bang, L. A. Becker, E. R. Frawley, S. Porwollik, H. F. Robbins, V. C. Thomas, R. Urbano, M. McClelland, F. C. Fang, The NsrR regulon in nitrosative stress resistance of *Salmonella enterica* serovar Typhimurium. *Mol. Microbiol.* **85**, 1179–1193 (2012).
52. Y. Seyoum, K. Baye, C. Humblot, Iron homeostasis in host and gut bacteria–A complex interrelationship. *Gut Microbes* **13**, 1874855–1874819 (2021).
53. K. Coppieters, T. Dreier, K. Silence, H. D. Haard, M. Lauwereys, P. Casteels, E. Beirnaert, H. Jonckheere, C. V. D. Wiele, L. Staelens, J. Hostens, H. Revets, E. Remaut, D. Elewaut, P. Rottiers, Formatted anti–tumor necrosis factor α VHH proteins derived from camelids show superior potency and targeting to inflamed joints in a murine model of collagen-induced arthritis. *Arthritis Rheum.* **54**, 1856–1866 (2006).
54. M. R. O'Brian, Perception and homeostatic control of iron in the rhizobia and related bacteria. *Annu. Rev. Microbiol.* **69**, 229–245 (2015).
55. G. Zhao, P. Ceci, A. Ilari, L. Giangiacomo, T. M. Laue, E. Chiancone, N. D. Chasteen, Iron and hydrogen peroxide detoxification properties of DNA-binding protein from starved cells: A ferritin-like DNA-binding protein of *Escherichia coli*. *J. Biol. Chem.* **277**, 27689–27696 (2002).
56. C. H. Goss, Y. Kaneko, L. Khuu, G. D. Anderson, S. Ravishankar, M. L. Aitken, N. Lechtzin, G. Zhou, D. M. Czyz, K. McLean, O. Olakanmi, H. A. Shuman, M. Teresi, E. Wilhelm, E. Caldwell, S. J. Salipante, D. B. Hornick, R. J. Siehnel, L. Becker, B. E. Britigan, P. K. Singh, Gallium disrupts bacterial iron metabolism and has therapeutic effects in mice and humans with lung infections. *Sci. Transl. Med.* **10**, eaat7520 (2018).
57. C. R. Fontenot, H. Tasnim, K. A. Valdes, C. V. Popescu, H. Ding, Ferric uptake regulator (Fur) reversibly binds a [2Fe-2S] cluster to sense intracellular iron homeostasis in *Escherichia coli*. *J. Biol. Chem.* **295**, 15454–15463 (2020).
58. H. Choi, Z. Yang, J. C. Weisshaar, Oxidative stress induced in *E. coli* by the human anti-microbial peptide LL-37. *PLOS Pathog.* **13**, e1006481 (2017).
59. Z. Z. Deris, J. Akter, S. Sivanesan, K. D. Roberts, P. E. Thompson, R. L. Nation, J. Li, T. Velkov, A secondary mode of action of polymyxins against Gram-negative bacteria involves the inhibition of NADH-quinone oxidoreductase activity. *J. Antibiot.* **67**, 147–151 (2014).
60. S. J. Dixon, B. R. Stockwell, The hallmarks of ferroptosis. *Annu. Rev. Cancer. Biol.* **3**, 35–54 (2019).
61. R. Ma, L. Fang, L. Chen, X. Wang, J. Jiang, L. Gao, Ferroptotic stress promotes macrophages against intracellular bacteria. *Theranostics* **12**, 2266–2289 (2022).
62. M. Conrad, V. E. Kagan, H. Bayir, G. C. Pagnussat, B. Head, M. G. Traber, B. R. Stockwell, Regulation of lipid peroxidation and ferroptosis in diverse species. *Genes Dev.* **32**, 602–619 (2018).
63. X. Shen, R. Ma, Y. Huang, L. Chen, Z. Xu, D. Li, X. Meng, K. Fan, J. Xi, X. Yan, H. Koo, Y. Yang, J. Jiang, L. Gao, Nano-decocted ferrous polysulfide coordinates ferroptosis-like death in bacteria for anti-infection therapy. *Nano Today* **35**, 100981 (2020).
64. F. E.-C. Jen, I. M. El-Deeb, Y. M. Zalucki, J. L. Edwards, M. J. Walker, M. von Itzstein, M. P. Jennings, A drug candidate for Alzheimer's and Huntington's disease, PBT2, can be repurposed to render Neisseria gonorrhoeae susceptible to natural cationic antimicrobial peptides. *J. Antimicrob. Chemother.* **76**, 2850–2853 (2021).
65. D. M. P. D. Oliveira, B. M. Forde, M.-D. Phan, B. Steiner, B. Zhang, J. Zuegg, I. M. El-deeb, G. Li, N. Keller, S. Brouwer, N. Harbison-Price, A. J. Cork, M. J. Bauer, S. F. Alquethamy, S. A. Beatson, J. A. Roberts, D. L. Paterson, A. G. McEwan, M. A. T. Blaskovich, M. A. Schembri, C. A. McDevitt, M. V. Itzstein, M. J. Walker, Rescuing tetracycline class antibiotics for the treatment of multidrug-resistant *Acinetobacter baumannii* pulmonary infection. *mBio* **13**, e03517–e03521 (2022).
66. K. A. Datsenko, B. L. Wanner, One-step inactivation of chromosomal genes in *Escherichia coli* K-12 using PCR products. *Proc. Natl. Acad. Sci. U.S.A.* **97**, 6640–6645 (2000).
67. Z. X. Zhong, Z. H. Cui, X. J. Li, T. Tang, Z. J. Zheng, W. N. Ni, L. X. Fang, Y. F. Zhou, Y. Yu, Y. H. Liu, X. P. Liao, J. Sun, Nitrofurantoin combined with amikacin: A promising alternative strategy for combating MDR uropathogenic *Escherichia coli*. *Front. Cell. Infect. Microbiol.* **10**, 608547 (2020).
68. F. C. Odds, Synergy, antagonism, and what the chequerboard puts between them. *J. Antimicrob. Chemother.* **52**, 1 (2003).
69. T. Wang, Y. Cui, J. Jin, J. Guo, G. Wang, X. Yin, Q. Y. He, G. Zhang, Translating mRNAs strongly correlate to proteins in a multivariate manner and their translation ratios are phenotype specific. *Nucleic Acids Res.* **41**, 4743–4754 (2013).
70. G. Bindea, B. Mlecnik, H. Hackl, P. Charoentong, M. Tosolini, A. Kirilovsky, W. H. Fridman, F. Pages, Z. Trajanoski, J. Galon, ClueGO: A Cytoscape plug-in to decipher functionally grouped gene ontology and pathway annotation networks. *Bioinformatics* **25**, 1091–1093 (2009).
71. K. J. Livak, T. D. Schmittgen, Analysis of relative gene expression data using real-time quantitative PCR and the 2−ΔΔCT Method. *Methods* **25**, 402–408 (2001).
72. F. Ruan, J. Zeng, H. Yin, S. Jiang, X. Cao, N. Zheng, C. Han, C. Zhang, Z. Zuo, C. He, RNA m6A modification alteration by black phosphorus quantum dots regulates cell ferroptosis: Implications for nanotoxicological assessment. *Small Methods* **5**, 2001045 (2021).
73. S. D. Taylor, J. Liu, X. Zhang, B. W. Arey, L. Kovarik, D. K. Schreiber, D. E. Perea, K. M. Rosso, Visualizing the iron atom exchange front in the Fe(II)-catalyzed recrystallization of goethite by atom probe tomography. *Proc. Natl. Acad. Sci. U.S.A.* **116**, 2866–2874 (2019).
74. R. Gao, A. M. Stock, Probing kinase and phosphatase activities of two-component systems in vivo with concentration-dependent phosphorylation profiling. *Proc. Natl. Acad. Sci. U.S.A.* **110**, 672–677 (2013).
75. L. Li, Y.-B. Su, B. Peng, X.-X. Peng, H. Li, Metabolic mechanism of colistin resistance and its reverting in *Vibrio alginolyticus*. *Environ. Microbiol.* **22**, 4295–4313 (2020).
76. X. Xiao, F. Zeng, R. Li, Y. Liu, Z. Wang, Subinhibitory concentration of colistin promotes the conjugation frequencies of *mcr-1*-and bla_{NDM-5}-positive plasmids. *Microbiol. Spectrum* **10**, e02160–e02121 (2022).
77. L. Han, X. W. Liu, T. Zang, H. Ren, D. S. Liang, S. C. Bai, C. Li, X. P. Liao, Y. H. Liu, C. Zhang, J. Sun, H_2S responsive PEGylated poly (lipoic acid) with ciprofloxacin for targeted therapy of *Salmonella*. *J. Control. Release* **351**, 896–906 (2022).
78. S. W. Jang, X. Liu, M. Yepes, K. R. Shepherd, G. W. Miller, Y. Liu, W. D. Wilson, G. Xiao, B. Blanchi, Y. E. Sun, K. Ye, A selective TrkB agonist with potent neurotrophic activities by 7,8-dihydroxyflavone. *Proc. Natl. Acad. Sci. U.S.A.* **107**, 2687–2692 (2010).

Acknowledgments: We thank R. Zhang (Second Affiliated Hospital of Zhejiang University) for the clinical isolate with colistin resistance mediated by *mgrB* mutation as a gift. We thank Z.-j. Zheng for critically reading this manuscript. **Funding:** This work was supported by Guangdong Major Project of Basic and Applied Basic Research (grant 2020B0301030007), the Foundation for Innovative Research Groups of the National Natural Science Foundation of China (32121004), Local Innovative and Research Teams Project of Guangdong Pearl River Talents Program (2019BT02N054), National Natural Science Foundation of China (32102720 and 32172909), Laboratory of Lingnan Modern Agriculture Project (NT2021006), Natural Science Foundation of Guangdong Province (2021A1515011079), Innovation Team Project of Guangdong University (2019KCXTD001), and the 111 Project (grant D20008). **Author contributions:** Conceptualization: J.S., H.R., Y.-h.L., and X.-p.L. Methodology: Z.-x.Z., S.Z., Y.-j. L., Y.-y.W., and Y.L. Investigation: Z.-x. Z., T.-f.L., Q.H., M.-y.L., Y.-f.Z., Y.Y., and L.-x.F. Visualization: H.R. and Z.-x.Z. Funding acquisition: J.S., H.R., Y.-f.Z., and Y.-h.L. Supervision: J.S. and H.R. Writing—original draft: H.R. and Z.-x.Z. Writing—review and editing: J.S., H.R., Z.-x.Z., B.N.K., and L. C. **Competing interests:** J.S., H.R., Z.-x.Z., and S.Z. are coinventors on a patent associated with this work, entitled "Application of 7,8-dihydroxyflavone synergize with colistin as iron homeostasis disruptor," reference number 202211500686.1. The other authors declare that they have no competing interests. **Data and materials availability:** All data needed to evaluate the conclusions in the paper are present in the paper and/or the Supplementary Materials.

Submitted 22 December 2022
Accepted 4 May 2023
Published 9 June 2023
10.1126/sciadv.adg4205